Supplementary Materials for

The cross-bridge spring: can cool muscles store elastic energy?

N.T. George, T.C. Irving, C.D. Williams, and T.L. Daniel*
*Correspondence to: danielt@uw.edu (T.L.D.)

Materials and Methods

Moths

Manduca sexta (L.) were raised in a colony maintained by the Department of Biology at the University of Washington, Seattle, WA, USA. After eclosion, moths were kept in light for 24 h. Moths were used within 5 days of eclosion. Prior to experimental preparation moths were immobilized by cold (~4ºC).

Work-loop preparation

Work-loop methods are as previously described in George et al., 2012 (13). In brief, the DLM_1 of *M. sexta* was subjected to sinusoidal length changes and phase-specific stimulation, while force output and length were recorded to calculate net work (Fig. 1). *M. sexta* (head, wings, and legs removed) were mounted in the work-loop apparatus, such that just the DLM_1 was isolated between a rigid force transducer (Fort100, WPI, Sarasota, FL, USA) and a motor lever arm (Model 305B Dual-Mode Lever Arm System, Aurora Scientific Inc., Aurora, ON, Canada). The muscle was electrically stimulated and sinusoidally oscillated at 25 Hz for 2 s. Two tungsten electrodes (~10 mm long) connected to a stimulator and driven through the DLM_1 (Isolator Pulse Stimulator Model 2100, A-M Systems, Sequim, WA, USA) delivered 0.4 ms supramaximal stimuli at the *in vivo* phase of activation, ~0.51 of the length cycle. The phase of activation was calculated as the duration of time from the start of muscle lengthening to the subsequent evoked potential as a fraction of the complete cycle duration (40 ms). The evoked potentials were recorded with a bipolar differential tungsten electrode inserted in the DLM_1 and a common reference wire placed in the abdomen. The signal was amplified (x1000) with a differential AC amplifier (Model 1800, A-M Systems, Sequim, WA, USA) and band pass filtered (300-20KHz). The induced peak-to-peak strain amplitude was ~0.6 mm (~±3% of the initial muscle length), with a duty factor of ~0.5 (the fraction of time spent shortening during the length cycle). The large inertial mass of *M. sexta's* body oscillating on the motor limited us to impose a strain only a fraction, ~60%, of the *in vivo* strain (19). To test for the effect of temperature, a heated *M. sexta* saline drip system maintained the muscle temperature at either 25 or 35ºC. The drip system included a temperature regulator (Bipolar Temperature Controller Model CL-100, Warner Instruments, Hamden, ST, USA), a cooling unit (Thermal Cooling Module Model TCM-1, Warner Instruments, Hamden, CT, USA), a pump (Masterflex C/L Mode l 77120-62, Cole-Parmer, Vernon Hills, IL, USA), and a drip emitter (In-line Heater/Cooler Model SC-20, Warner Instruments, Hamden, CT, USA).

Net work per cycle was calculated by integrating force output with respect to muscle length (Fig. 1B). For each experimental condition, we calculated the net work for 20 cycles, starting with the 10^{th} cycle. Mass specific power output is the product of mean net work and cycle frequency (25 Hz, normal wingbeat frequency) divided by the mass of the DLM_1. We determined the mass of the DLM_1 by extracting the muscle from the thorax while immersed in *M. sexta* saline directly after experimentation. The DLM_1 was then blotted and weighed to the nearest 0.1 mg. Power output by the DLM_1 was not confounded by a decrease in performance over the ~10 min experiment period due to fatigue. A prior work-loop study on *M. sexta* found no significant difference in power output after 20 min of work-loop testing under similar conditions (13).

X-ray diffraction

Time-resolved X-ray diffraction patterns were collected using the small-angle diffraction instrument on the Biophysics Collaborative Access Team beamline 18 ID at the Advanced Photon Source, Argonne National Laboratory. The work-loop apparatus was positioned to hold the preparation in the direct line of the X-ray beam, 2.945 m from the PILATUS 100K detector (Dectris, Ltd.). The X-ray beam contained ~1 x 10^{13} photons per second at 12 keV beam energy and was collimated to about 250 x 250 μm at the sample position and focused to ~50x150 μm at the detector. The stimulus signal sent to the DLM_1 also triggered the shutter driver acting as a gate and delay generator (Model VMM-T1, Uniblitz, Rochester, NY, USA) to open the slow X-ray shutter (model PFCU/PF4/PFS2 XIA LLC Hayward CA). A custom made fast shutter (~1 ms latency, < 1ms minimum opening time), gated by the PILATUS integration signal was triggered to open every 8 ms (with 4 ms exposures) of the 40 ms wingbeat cycle, yielding a total of 5 diffraction images per cycle for 100 cycles. This essentially produced a diffraction movie of 125 frames/s with each frame representing the phase-sensitive structure of the contractile unit. This is made possible by the one-to-one coupling of excitation and contraction in the synchronous flight muscles in these animals. Thus, muscle stimulation can be used to synchronize time-resolved X-ray diffraction images in intact preparations. The stage holding the work-loop apparatus was attached to a motor driven unit that rastered the sample horizontally (± 2 mm) at ~0.5 m/s during the X-ray exposure to limit the amount of radiation a single point in the muscle fiber received. In addition to testing for the effect of temperature, we also tested for an effect of DLM_1 subunit location. The sample was positioned such that the X-rays were incident on one of two locations, a dorsal and a ventral region of the DLM_1.

Diffraction pattern analysis

For each condition, 400 images were averaged across the corresponding phases of the length cycle to yield one cycle of 5 diffraction images, significantly improving the signal-to-noise ratio of the image. When cross-bridges move from the region of the thick filament backbone to that of the thin filament, there is an increase in the mass along the 2,0 crystallographic plane (only thin filaments) and a reduction in mass along the 1,0 plane (thick and thin filaments). The 1,1 reflection is a weak one that cannot always be resolved from the much stronger 2,0 reflection (17). As such, the ratio of the intensities of the 2,0 + 1,1, and 1,0 equatorial reflections ($I_{1,1}+I_{2,0}/I_{1,0}$) can be used as a measure of the radial position of cross-bridges relative to the thick and thin filament (Fig. 1). The equatorial intensity ratio reflects the mass shift of cross-bridges as they move away from the thick filament towards the thin filament;

higher ratios reflect increased radial extension, presumably associated with acto-myosin interaction (17, 20).

Using custom written software in Python, we determined the intensities of the 2,0, 1,1 and 1,0 reflections ($I_{2,0}$, $I_{1,1}$, and $I_{1,0}$), by first integrating the intensities orthogonal to the equatorial line. An exponential fit based on manually selected points along the baseline removed the diffuse background. The area under the one dimensional projection of $I_{2,0}$, $I_{1,1}$, and $I_{1,0}$ was then calculated by peak fitting using Fityk (22) assuming a Gaussian shape and the peak positions constrained to be at the expected reciprocal lattice positions and peak widths constrained as described by Yu et al. 1985 (23). Briefly, the width of the Gaussian representing a given diffraction peak $\sigma_{h,k}$ can be expressed as:

$$\sqrt{\sigma_c^{\,2} + \sigma_d^{\,2} S_{h,k} + \sigma_s^{\,2} S_{h,k}^{\,2}},$$

where $S_{h,k} = \sqrt{h^2 + k^2 + hk}$ and h and k are the Miller indices of the diffraction peak. σ_c is the known width of the X-ray beam (~ 1 pixel), σ_d is related to the amount of heterogeneity in inter-filament spacing among the myofibrils, and σ_s is related to the amount of paracrystalline (liquid-like) disorder of the myofilaments in the hexagonal lattice. Both σ_d and σ_s are used as free parameters of the fits. If the cool dorsal region of the muscle behaves as a lattice of elastic elements we would expect that the cross-bridges are on average more associated with the thin filament throughout the contraction cycle. In contrast, we expect warmer ventral muscles to behave as the main power generators and therefore to have greater cross-bridge turnover. This would correspond with a comparatively stable intensity ratio in cool muscle versus a periodically fluctuating intensity ratio in warm muscle. Additionally, we were able to track lattice spacing by measuring the distance between the 1,0 equatorial reflection and the center of the pattern. This was converted to the d_{10} lattice spacing, the distance between myofilaments, as in Irving, 2006 (20).

Data acquisition

Force, muscle length, evoked potentials, and shutter exposures were recorded at 5000 Hz by a data acquisition system (NI USB-6229, National Instruments, Austin, TX, USA) and relayed to a central processing unit. Evoked potentials were analyzed using custom peak detection software in MATLAB developed by M. S. Tu (University of Washington, Seattle, WA, USA).

Operating conditions

The 5 moths (2 males and 3 females) used in these trials had a mean body mass of 2.50±0.17 g and a mean extracted DLM_1 mass of 0.206±0.009 g (s.d). The mean rest length of the mesothorax was 10.07±0.14 mm (s.d.), which set the mean operating mesothorax length at 9.86±0.14 mm (s.d.). The mean peak-to-peak strain amplitude imposed by the motor on the DLM_1 was 0.63±0.02 mm (s.d.), with only 1.1% strain amplitude variation across individuals. The DLM_1 was electrically stimulated near the *in vivo* phase of activation, 0.51±0.01 (approximately halfway into the cycle) (19).

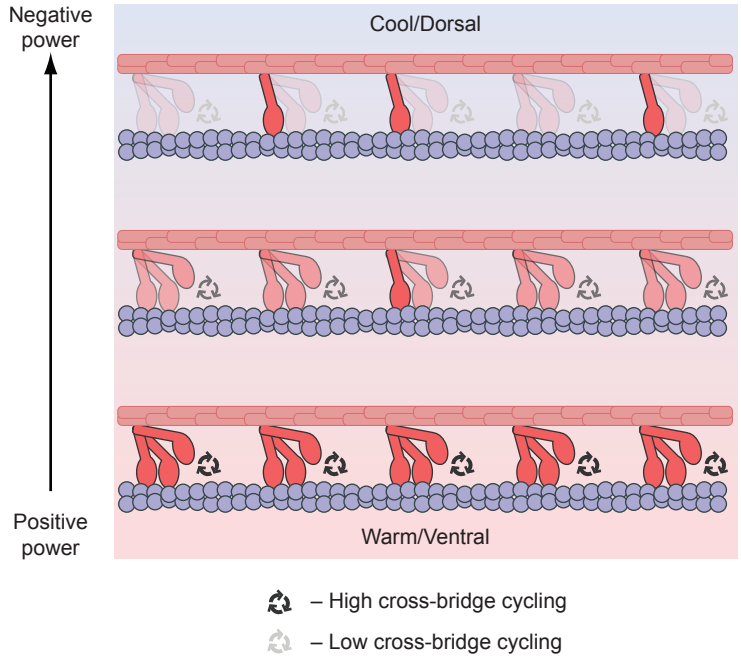

Fig. S1.

A schematic showing a gradient in molecular cycling dynamics resulting from a temperature gradient. Following the proposed temperature gradient in *M. sexta*, power output would vary significantly from positive power output in the warm sectors to zero power output (elastic behavior) and then negative power output (damping behavior) in the cooler sectors. Muscle activation and deactivation rates significantly depend on temperature, therefore cross-bridge cycling rates will also vary along the temperature gradient from high cycling in warm regions to low cycling in the cooler regions. Because of the decrease in cross-bridge cycling rates associated with the decrease in temperature, cross-bridges in the cooler region of muscle have an increased likelihood of remaining bound to their actin binding site for a longer period of time (darker red bound cross-bridge). Elastic energy stored in cross-bridges that remain bound and deformed at the extrema of the lengthening and shortening phase of the contraction cycle could be released upon detachment at the start of the subsequent phase. In doing so, the deformed cross-bridges aid the antagonistic muscle by acting as a restoring force.

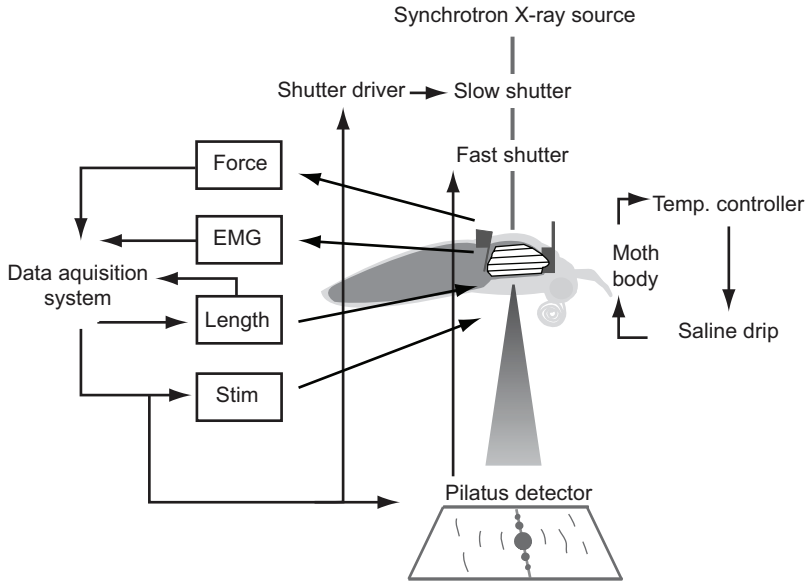

Fig. S2.

Experimental system. We cyclically lengthened and electrically stimulated the DLM_1 at the *in vivo* phase of activation, while recording force output, evoked potentials, and length. A shutter, synchronized to the first muscle stimulus, performed a 4 ms exposure every 8 ms. Saline maintained the muscle at 25 or 35ºC.

Movie S1

An animation consisting of 5-frame X-ray diffraction movies (on the right) paired with their respective mechanical measures of force and length (creating a work-loop, on the left), one from the 25ºC condition and one from the 35ºC condition. X-ray diffraction images from concurrent points in the contraction cycle highlight the temperature dependent variation in muscle lattice structure. The effect of temperature on cross-bridge mass shift is observed as a difference in the relative intensities of the 1,0, 1,1, and 2,0 equatorial reflections and the change in lattice spacing is indicated by the difference in distance between opposing 1,0 equatorial reflections.